J. Fluid Mech. (1992), *vol.* 242, *pp.* 79–98
Printed in Great Britain

Effects of horizontal gradients on thermohaline instabilities in infinite porous media

By ALOK SARKAR† AND O. M. PHILLIPS
Department of Earth and Planetary Sciences, Johns Hopkins University, Baltimore, MD 21218, USA

(Received 17 May 1991 and in revised form 5 February 1992)

Thermohaline instabilities produced by horizontal gradients of temperature and salinity in a saturated homogeneous isotropic infinite porous medium are studied using linear stability analysis. In the basic state horizontal gradients of temperature and salinity are taken to be mutually compensating, so that the basic-state fluid density does not vary horizontally. It is found that under these conditions the fluid is always unstable. In a porous medium, assuming the solid matrix to be impervious to dissolved salts, the effective advection rates of heat and dissolved salts are different. Because of this difference any disturbance involving a horizontal component of displacement creates net horizontal density gradients, and thus destabilizes the predominantly hydrostatic force balance. When the vertical Rayleigh number is positive, the typical velocity field consists of almost vertical layers of fluid sliding past each other in opposite directions (salt fingers). When the vertical Rayleigh number is negative the fluid layers are almost horizontal, similar to the interleaving observed in Newtonian fluids. Resulting perturbation fluxes of heat and salt always tend to reduce the basic-state concentration gradients, and typically also the gravitational potential energy of the fluid. We also make some tentative estimates regarding properties of these instabilities at the fully developed state. It seems that thermohaline fine structures, similar to oceanic observations, are also possible in porous media.

1. Introduction

Thermohaline instabilities in porous media play important roles in many geologically significant phenomena. For example Phillips (1991, §5.4) proposed 'salt fingering' beneath hypersaline lagoons as a possible mechanism of dolomitization of limestones. Griffiths (1981) suggested the presence of a 'diffusive interface' at the bottom of the Earth's crust to explain the separation of hot brine from convecting ground water in the Wairakei geothermal system. Bischoff & Rosenbauer (1989) postulated the presence of deep-seated 'diffusive interfaces' within the oceanic crust to explain salinity variations in vent fluids of seafloor geothermal systems. Lindblom (1986) proposed that mixing prompted by double-diffusive instabilities resulted in deposition of sulphides and fluorites at Laisvall, Sweden. Evans & Nunn (1989) found that thermohaline effects were crucial in explaining inferred groundwater flow patterns near salt domes. Similar physical mechanisms are also potentially important in groundwater contamination, where the chemically laden water will play the role of salty water. Gradients of fluid temperature and salinity are hardly ever perfectly

† Present address: Department of Geology and Geophysics, Louisiana State University, Baton Rouge, LA 70803, USA

vertical in a natural situation. In some situations, e.g. near a salt dome (Bennett & Hanor 1987), the horizontal components of property gradients are just as strong as vertical gradients. In this paper we examine consequences of the presence of these horizontal gradients on characteristics of thermohaline instabilities in a saturated homogeneous isotropic infinite porous medium.

The first theoretical analysis of double-diffusive instability in porous media was apparently done by Nield (1968). He considered the case of purely vertical property gradients. To our knowledge nobody has looked at the effect of horizontal gradients on double-diffusive instabilities in porous media, although a similar analysis has been done for a Newtonian fluid. Thorpe, Hutt & Soulsby (1969) reported an approximate analysis of the linear stability boundary for horizontal and vertical fluid layers of finite thickness. The accuracy of their solution increased asymptotically with increase in the magnitudes of horizontal and vertical Rayleigh numbers. They concluded that the presence of horizontal gradients was strongly destabilizing, though a large negative vertical Rayleigh number could make the situation stable. Subsequently Hart (1971) reported an accurate numerical solution of the stability boundary for a vertical column of salt-stratified fluid heated from a sidewall. Paliwal & Chen (1980) reported a similar numerical analysis for fluid layers of varying inclinations. These analyses concentrated on accurately incorporating laboratory boundary conditions in the calculation of the stability boundary. By contrast Holyer (1983) assumed the depth of the fluid layer to be infinite and obtained detailed results regarding the behaviour of the most unstable modes. In the present paper we take the second approach.

The first laboratory experiments on double-diffusive convection in porous media were reported by Griffiths (1981). He showed that if a salt-stratified saturated porous layer is heated from below, it forms sharp 'diffusive interfaces' similar to those in a Newtonian fluid. Imhoff & Green (1988) showed the existence of 'salt fingers' in a porous medium. Murray & Chen (1989) experimentally studied the onset of thermohaline convection in porous media. In all these studies the thermohaline gradients were maintained vertical. No porous media experiments seem to have been done with horizontal property variations but experiments done in a Newtonian fluid may provide some guidance. Flow visualization studies of Thorpe *et al.* (1969) clearly showed the onset and growth of horizontal interleaving. Similar experimental observations were made by Wirtz, Briggs & Chen (1972), Ruddick & Turner (1979), Holyer *et al.* (1987) and others.

2. Linear stability analysis

We consider a homogeneous saturated porous medium of infinite extent. We assume that at the initial state the fluid is quiescent. The isothermal and isohaline surfaces are assumed to be inclined and straight, with the restriction that horizontal gradients of temperature and salinity are mutually compensating such that the fluid density does not vary in the horizontal direction. This restriction is necessary since the presence of a net horizontal density gradient will not be dynamically consistent with the assumption of an initial state of rest. Interestingly, the higher thermal conductivity of salt compared to that of geological sediments do tend to produce compensating horizontal thermohaline gradients near a salt dome (Evans & Nunn 1989). The assumption that isotherms and isohalines are straight is necessitated by the fact that at the initial state diffusive fluxes of heat and salt should be constant. The density may vary in the vertical direction. We find the (x, z)-plane as the vertical

plane along which the horizontal gradients of temperature, and hence salinity, are the steepest. We show in Appendix A that the Squires theorem holds for this problem, hence disturbances confined to the (x, z)-plane are always more unstable than their three-dimensional counterparts. Therefore in the following discussion we will assume that all motion is two-dimensional. The z-axis is taken to be positive vertically upwards and the sense of the x-axis is chosen so that the basic-state horizontal salinity and temperature gradients are positive.

For an infinite-medium problem the lengthscale is to be determined from properties of the medium. For problems of thermal and thermohaline instabilities the only relevant dimensional property of the saturated porous medium is its hydraulic conductivity $K(= k_p g/\nu)$, where k_p is the permeability of the medium, g is the acceleration due to gravity and ν is the kinematic viscosity of the fluid. Apparently, the intrinsic lengthscale of the problem is $l^* = k_\theta/K$, where k_θ is the effective thermal diffusivity of the saturated medium. Similarly the intrinsic timescale is $t^* = k_\theta/K^2$. For a water-saturated porous medium of permeability one darcy $l^* \approx 1.4$ cm and $t^* \approx 23$ min. We will be treating the porous medium as a continuum. For this to be valid it is necessary that the lengthscale of the problem be much larger than the typical grain size. Typically $k_p \sim 10^{-2}\phi\delta^2$ (Phillips 1991; §2.7), where ϕ is the porosity of the medium and δ is the r.m.s. grain size. When water is the interstitial fluid this implies that $\delta \ll l^*$ only if $k_p \ll 100$ darcy. This restriction will exclude very high-permeability media like gravel, karst limestone and clean sand from the domain of applicability of the present analysis. For media with permeability of 1 darcy or higher, lengthscales of disturbances with positive growth rates are at least one order of magnitude larger than l^*. This relaxes the above restriction quite a bit. In the following discussion all length and time variables are scaled by l^* and t^* respectively. Mathematically the basic state is described as

$$\left.\begin{aligned} T^0(x,z) &= T_r + T_x^0 x + T_z^0 z, \\ S^0(x,z) &= S_r + S_x^0 x + S_z^0 z, \\ \alpha T_x^0 &= \beta S_x^0, \\ \rho^0(z) &= \rho_0[1-(\alpha T_z^0 - \beta S_z^0) z], \end{aligned}\right\} \tag{1}$$

where

$$\alpha = -\frac{1}{\rho}\left(\frac{\partial\rho}{\partial T}\right)_S, \quad \beta = \frac{1}{\rho}\left(\frac{\partial\rho}{\partial S}\right)_T$$

so that α and β both are positive.

To obtain the disturbance equations we add dynamically permissible perturbations of physical quantities to the basic state. We assume perturbations to be small compared to corresponding basic-state quantities and hence neglect products of perturbation quantities. The appropriate momentum equation for a single-phase fluid in a saturated, homogeneous and isotropic porous medium is the Darcy's law. Combining Darcy's law with the Boussinesq approximation (incompressibility condition) and the linearized equation of state one obtains

$$\nabla^2\Psi' = -\left(\alpha\frac{\partial T'}{\partial x} - \beta\frac{\partial S'}{\partial x}\right). \tag{2}$$

Primes denote disturbance quantities. The stream function is defined such that

$$u'(x,z,t) = \frac{\partial\Psi'}{\partial z}, \quad v'(x,z,t) = -\frac{\partial\Psi'}{\partial x},$$

where (u', v') is the transport velocity (not the pore velocity) of the fluid. Neglecting dissipative, chemical or other sources of heat generation one obtains the linearized equation of heat conservation:

$$\frac{\partial T'}{\partial t}+\frac{1}{\Gamma}\left(\frac{\partial \Psi'}{\partial z}T_x^0-\frac{\partial \Psi'}{\partial x}T_z^0\right)=\nabla^2 T', \tag{3}$$

where Γ is the ratio of volumetric heat capacity of the saturated matrix to that of the fluid. Assuming neither any loss of salt by precipitation or crystallization nor any gain by dissolution of the solid matrix, one obtains the linearized salt balance equation:

$$\frac{\partial S'}{\partial t}+\frac{1}{\phi}\left(\frac{\partial \Psi'}{\partial z}S_x^0-\frac{\partial \Psi'}{\partial x}S_z^0\right)=\tau\nabla^2 S', \tag{4}$$

τ is the ratio of the effective molecular diffusivity of salt in the fluid (taking into account the effect of fluid path tortuosity) to the effective (molecular) thermal diffusivity of the saturated matrix. The inverse of τ is called Lewis number. Typically τ is of order 10^{-2}. Equations (2), (3) and (4) together constitute the final set of disturbance equations. Since the medium is infinite there are no formal boundary conditions, the only requirement is that disturbance quantities remain bounded everywhere. Typically $\Gamma \approx 1$, hence the advection rate of heat is $\approx u$. In contrast, the porosity of the medium $\phi \ll 1$, so that the advection rate of salt, u/ϕ, is much larger than that of heat. This difference between advection rates of two components which affect the fluid density is primarily responsible for the instability described in this paper. This is similar to but different from the double-*diffusive* instability observed in Newtonian fluids. This mechanism of instability has been called double-*advective* instability (Phillips 1991). In addition, the fact that $\tau \ll 1$ opens the door for the double-diffusive mechanism to destabilize the situation even more. Nevertheless double-advective effects are predominant.

Equations (2), (3) and (4) can be reduced to a single equation as:

$$\left(\nabla^2-\frac{1}{\tau}\frac{\partial}{\partial t}\right)\left(\nabla^2-\frac{\partial}{\partial t}\right)\nabla^2\Psi'=R_x\frac{\partial^2}{\partial x\,\partial z}(\nabla^2\Psi')-R_z\frac{\partial^2}{\partial x^2}(\nabla^2\Psi')-\frac{1}{\tau}\frac{\partial}{\partial t}\left(W_z\frac{\partial^2\Psi'}{\partial x\,\partial z}-W_z\frac{\partial^2\Psi'}{\partial x^2}\right), \tag{5}$$

where

$$R_x=\frac{k_\theta \nu}{k_p g}\left(\frac{\beta S_x^0}{\phi\tau}-\frac{\alpha T_x^0}{\Gamma}\right), \quad R_z=\frac{k_\theta \nu}{k_p g}\left(\frac{\beta S_z^0}{\phi\tau}-\frac{\alpha T_z^0}{\Gamma}\right),$$

$$W_x=\frac{k_\theta \nu}{k_p g}\left(\frac{\beta S_x^0}{\phi}-\frac{\alpha T_x^0}{\Gamma}\right), \quad W_z=\frac{k_\theta \nu}{k_p g}\left(\frac{\beta S_z^0}{\phi}-\frac{\alpha T_z^0}{\Gamma}\right).$$

The right-hand sides of the above expressions are in the dimensional form. R_x and R_z are the horizontal and vertical Rayleigh numbers respectively. Notice that when one uses a diffusive lengthscale the Rayleigh numbers increase with increase in kinematic viscosity of the pore fluid. W_x and W_z are weighted horizontal and vertical concentration gradients respectively. The parameters W_x and W_z are unique to porous-media dynamics. In addition to the small-amplitude assumption we assume that the extent of the initial disturbance is limited in space, so that the Fourier transform of the disturbance with respect to spatial variables exists. This permits us to confine our attention to a single Fourier component of the disturbance at a time. Hence we assume solution of (5) of the form

$$\Psi'(x,z,t)=\psi_0 \exp\left[nt+\mathrm{i}(xl\cos\theta+zl\sin\theta)\right]. \tag{6}$$

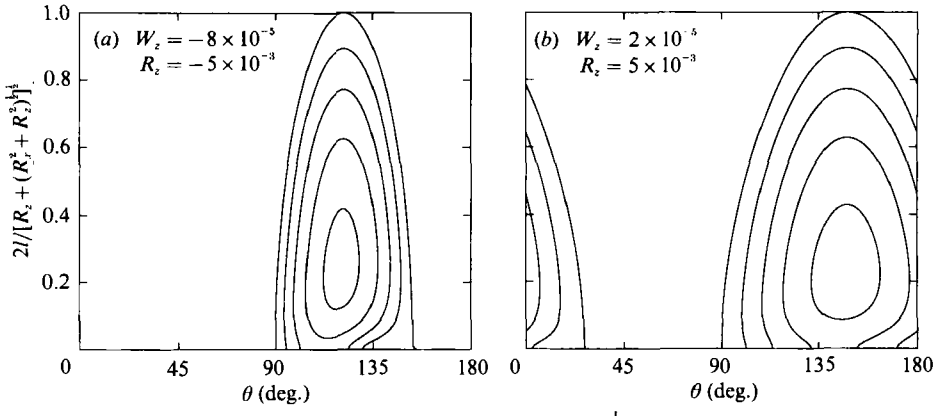

FIGURE 1. Contour plots of growth rate $2l/\tau[R_z+(R_x^2+R_z^2)^{\frac{1}{2}}]$. (*a*) A case which would have been stable in the absence of any horizontal gradient. The vertical gradients represented in (*b*) are unstable even in the absence of any horizontal gradients. The growth rate is scaled by an approximate expression of the peak growth rate (equation (26)), and the largest wavenumber with a non-negative growth rate (equation (10)) is used to scale the wavenumber. $W_x = 8\times10^{-5}$, $R_x = 10^{-2}$, $\tau = 10^{-2}$. Contour levels are 0, 0.2, 0.4, 0.6 and 0.8.

Substituting (6) in (5) one can derive the following equation for the disturbance growth rate:

$$n^2+n[l^2(1+\tau)-\tfrac{1}{2}(W_z(\cos 2\theta+1)-W_x\sin 2\theta)] + [\tau l^4-\tfrac{1}{2}\tau l^2(R_z(\cos 2\theta+1)-R_x\sin 2\theta)] = 0. \quad (7)$$

Using properties of quadratic equations it can be shown (Appendix B) that the real part of both roots (7) will be less than or equal to zero, i.e. the basic state will be stable only if both of the following conditions are satisfied:

$$R_z \leqslant \mu R_x + k^2(1+\mu^2)^2, \quad (8)$$

$$W_z \leqslant \mu W_x + k^2(1+\tau)(1+\mu^2)^2, \quad (9)$$

where $k(=l\cos\theta)$ is the horizontal component of the disturbance wavenumber and $\mu = \tan\theta$. Equations (8) and (9) are both necessary and sufficient. It can be shown (Appendix C) that if $(\mathrm{d}\rho/\mathrm{d}z) < 0$, then satisfaction of (8) implies satisfaction of (9). In the present paper we consider only the case of density decreasing with height, hence for us (8) is both a necessary and sufficient condition for stability. For given values of $R_x(\neq 0)$ and R_z one can always choose μ and k such that (8) is not satisfied. Hence, so long as $R_x \neq 0$, there are always some scales and modes of disturbances to which the basic state is unstable. One obtains similar result in a Newtonian fluid (Holyer 1983). Note that when $R_x = 0$, the situation is stable if $R_z \leqslant 0$. Obviously the presence of horizontal gradients is strongly destabilizing. It can be shown (Appendix C) that so long as $\mathrm{d}\rho/\mathrm{d}z < 0$, if the growth rate is complex its real part is necessarily negative. A different statement of the above result is that 'overstability' is not possible in the present case. In a porous medium inertial acceleration of the interstitial fluid is negligible compared to the viscous drag. This rules out the possibility of growing oscillations. By contrast, in an infinite fluid oscillatory modes can be growing with time, though usually the fastest growing modes are not oscillatory (Holyer 1983).

Examples of numerical solutions of (7) are shown in figure 1. These are contour plots of constant disturbance growth rates. Notice that (7) predicts two growth rates,

and only positive values of the higher one have been plotted. Note that there exists well-defined peak growth rate, that the peak growth rate is of the same order as the highest growth rate at the non-diffusive limit ($l = 0$) and that the most unstable orientations (θ) for different wavenumber magnitudes are quite close. In general the range of values of l and θ for positive growth rate increases with increase in values of W_x, W_z, R_x and R_z.

From (8) it is clear that for any given angle, θ, of the wavenumber vector, the largest wavenumber with non-negative growth rate is given by

$$l^2 = \tfrac{1}{2}[R_z(\cos 2\theta + 1) - R_x \sin 2\theta].$$

The largest wavenumber with non-negative growth rate is obtained by setting $\partial l/\partial\theta = 0$ in the above equation. The corresponding mode of disturbance (denoted by subscript m), satisfies the following relations:

$$l_{\mathrm{m}} = \frac{1}{\sqrt{2}}[R_z + (R_x^2 + R_z^2)^{\frac{1}{2}}]^{\frac{1}{2}}, \tag{10}$$

$$\sin(2\theta_{\mathrm{m}}) = -\frac{R_x}{(R_x^2 + R_z^2)^{\frac{1}{2}}}, \tag{11}$$

$$\cos(2\theta_{\mathrm{m}}) = \frac{R_z}{(R_x^2 + R_z^2)^{\frac{1}{2}}}. \tag{12}$$

Equation (10) may be interpreted as indicating that for a disturbance to be destabilizing, the Rayleigh number formed with the inverse of the disturbance wavenumber as the lengthscale should be of order one or larger. In a dimensional form the smallest lengthscale is given by

$$2\pi l_{\mathrm{m}}^{-1} \approx 8.9\left[\frac{\tau\phi k_\theta \nu}{k_p g[\beta S_z^0 + (\beta^2 S_z^{02} + \beta^2 S_x^{02})^{\frac{1}{2}}]}\right]^{\frac{1}{2}}.$$

For a water-saturated medium with $k_p = 1$ darcy, $\tau\phi = 0.005$, $\beta S_z^0 = \pm 1\,\%$ per 10 m and $\beta S_x^0 = 0.5\,\%$ per 10 m the smallest lengthscales ($2\pi l_{\mathrm{m}}^{-1}$) are about 160 cm (for $\beta S_z^0 > 0$) and 750 cm (for $\beta S_z^0 < 0$).

3. The non-diffusive limit

For a disturbance of finite size, $l = 0$ implies that $l^* = k_\theta/C = 0$, i.e. it corresponds to the non-diffusive limit. For a disturbance of the form of (6) the growth rate in this limit is

$$n = \frac{W_z - \mu W_x}{1 + \mu^2} \tag{13}$$

and it is independent of the disturbance lengthscale. (Note that though we are discussing the non-diffusive limit, for ease of comparison with other sections, we still use the diffusive lengthscale. The form of equations remain unchanged by changes in the lengthscale.) The largest growth rate (denoted by subscript 0) is given by

$$n_0 = \tfrac{1}{2}[W_z + (W_x^2 + W_z^2)^{\frac{1}{2}}]. \tag{14}$$

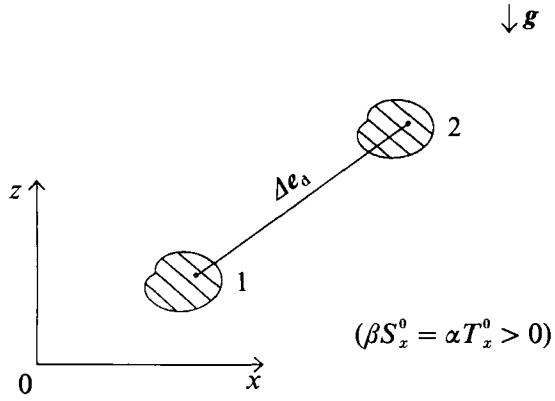

FIGURE 2. Displacement of a fluid parcel from point 1 to 2. This diagram also shows the orientation of the coordinate system.

The most unstable orientation (θ_0, see (6)) of the wavenumber vector is given by

$$\sin(2\theta_0) = -\frac{W_x}{(W_x^2+W_z^2)^{\frac{1}{2}}}, \tag{15}$$

$$\cos(2\theta_0) = \frac{W_z}{(W_x^2+W_z^2)^{\frac{1}{2}}}. \tag{16}$$

For a water-saturated medium with $k_p = 1$ darcy, $\phi = 0.15$, $\beta S_z^0 = \pm 1\%$ per 10 m and $\beta S_x^0 = 0.5\%$ per 10 m the timescales for disturbance growth rate (n_0^{-1}) are approximately 6 months (for $\beta S_z^0 > 0$) and 8 years (for $\beta S_z^0 < 0$).

From (13) it is clear that in the non-diffusive limit disturbance growth rates are always real. Making use of the definition of the stream function one can recast (13) in the dimensional form

$$n = \frac{K}{\phi}(\boldsymbol{e}_d \cdot \boldsymbol{e}_z)\left(\boldsymbol{e}_d \cdot \nabla\left(\beta S^0 - \frac{\phi \alpha T^0}{\Gamma}\right)\right), \tag{17}$$

where $\boldsymbol{e}_z$ and $\boldsymbol{e}_d$ are unit vectors pointing vertically upwards and in the direction of the displacement respectively. Equation (17) can provide a quantitative account of physical processes responses responsible for instability in the non-diffusive limit. Let the displacement of a parcel of fluid be Δ (figure 2). Let the basic-state temperature (salinity) of the fluid at the initial and final locations be T_1 and T_2 (S_1 and S_2) respectively. Obviously, $T_2 - T_1 = (\boldsymbol{e}_d \nabla T^0)\Delta$ and $S_2 - S_1 = (\boldsymbol{e}_d \cdot \nabla S^0)\Delta$. Let the temperature and salinity of the fluid parcel at the displaced position, after necessary adjustment, be $\hat{T}$ and $\hat{S}$ respectively. Conservation of salt requires that $\hat{S} = S_1$. Similarly $\hat{T}$ can be evaluated from heat balance equation per unit volume of the saturated matrix:

$$[(1-\phi)(\rho c)_s + \phi(\rho c)_f]T_1 + (\rho c)_s(1-\phi)T_2 = (1-\phi)(\rho c)_s T_1 + [(1-\phi)(\rho c)_s + \phi(\rho c)_f]\hat{T}.$$

Which upon simplification yields:

$$(T_2 - \hat{T}) = \frac{\phi}{\Gamma}(T_2 - T_1) = \frac{\phi}{\Gamma}(\boldsymbol{e}_d \cdot \nabla T^0)\Delta,$$

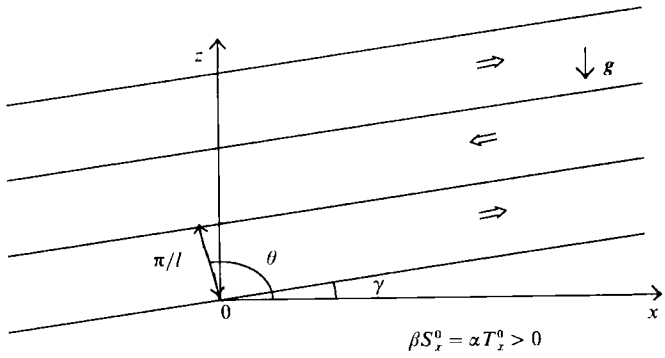

FIGURE 3. Typical disturbance velocity field. Notice that the direction of fluid motion is perpendicular to the wavenumber vector.

where $\Gamma = [(1-\phi)(\rho c)_s + \phi(\rho c)_f]/(\rho c)_f$. Hence the buoyancy force acting per unit volume of the displaced fluid is $g\rho_0 \Delta(\boldsymbol{e}_d \cdot \nabla(\beta S^0 - \phi\alpha T^0/\Gamma))$. Only the component of this force in the direction of the displacement determines the linear stability of the basic state. Equating the pore velocity of the fluid to $n\Delta$, using Darcy's law and the fact that the transport velocity of the fluid is ϕ times its pore velocity one obtains an alternative derivation of (17).

Equations (15) and (16) imply that the direction of fluid motion corresponding to the most unstable mode are limited to the first and third quadrants (where S^0 and T^0 are taken to increase to the right, figure 3). This is similar to theoretical predictions (Holyer 1983) and experimental observations (Thorpe *et al.* 1969) in Newtonian fluids. If the horizontal component of the displacement of a fluid parcel is towards the hotter and saltier region (i.e. towards the positive x-direction), then following arguments from the above paragraph one can show that, being substantially less saline but only slightly cooler, it will be lighter than the surrounding fluid. Hence the original displacement will be unstable only when its vertical component is upwards, explaining why most unstable displacements are confined to the first and third quadrants. Later it will be clear that, so long as $(\alpha T_z^0/\beta S_z^0 - 1)\phi/\Gamma \ll 1$, the same is true for the diffusive case.

4. The most unstable mode for given gradients

One can determine the most unstable growth rate and the corresponding mode of disturbance from (7) by setting $\partial n/\partial l = \partial n/\partial\theta = 0$. The fact that n is always real for unstable modes (so long as $(\mathrm{d}\rho/\mathrm{d}z) < 0$) simplifies the algebra. The peak growth rate and the wavenumber magnitude are given by

$$n_p = \frac{\tau[R_z(\cos 2\theta_p + 1) - R_x \sin 2\theta_p][R_x + R_z \tan 2\theta_p]}{2[(1+\tau)(R_x + R_z \tan 2\theta_p) - 2(W_x + W_z \tan 2\theta_p)]}, \tag{18}$$

$$l_p^2 = \frac{[R_x \sin 2\theta_p - R_z(\cos 2\theta_p + 1)][W_x + W_z \tan 2\theta_p]}{2[(1+\tau)(R_x + R_z \tan 2\theta_p) - 2(W_x + W_z \tan 2\theta_p)]} \tag{19}$$

and the angle of the wavenumber vector is determined from

$$B_p^2[(1+\tau)M_p - \tau N_p] - 2M_p B_p A_p + N_p A_p^2 = 0, \tag{20}$$

where the subscript p corresponds to the peak growth rate and

$$\left.\begin{aligned} A_{\mathrm{p}} &= W_x + W_z \tan 2\theta_{\mathrm{p}}, \quad B_{\mathrm{p}} = R_x + R_z \tan 2\theta_{\mathrm{p}}, \\ M_{\mathrm{p}} &= W_x \sin 2\theta_{\mathrm{p}} - W_z(\cos 2\theta_{\mathrm{p}} + 1), \quad N_{\mathrm{p}} = R_x \sin 2\theta_{\mathrm{p}} - R_z(\cos 2\theta_{\mathrm{p}} + 1). \end{aligned}\right\} \tag{21}$$

4.1. *An approximate solution*

Analytic solutions of n_{p}, l_{p} and θ_{p}, in terms of basic-state property gradients (from the equation set (18)–(20)) are apparently impossible to derive. Nevertheless it can be shown that $R_x = W_x(1-\tau\hat{\phi})/[\tau(1-\hat{\phi})]$ and $R_z = W_z(1-r\tau\hat{\phi})/[\tau(1-r\hat{\phi})]$, where $r = \alpha T_z^0/\beta S_z^0$ and $\hat{\phi} = \phi/\Gamma$. Now, $\tan 2\theta_{\mathrm{m}} - \tan 2\theta_0 = W_x/W_z - R_x/R_z = (W_x/W_z)\hat{\phi}(1+\tau)(r-1)/[(1-\hat{\phi})(1-r\tau\hat{\phi})]$. Typically $r = O(1)$, $\hat{\phi} \leqslant O(0.1)$ and $\tau = O(10^{-2})$. Hence assuming $(r-1)\hat{\phi} \ll 1$ and $W_x/W_z \leqslant O(1)$ one obtains

$$|\theta_0 - \theta_{\mathrm{m}}| = O\left(\frac{R_x}{R_z}\phi\right) \ll 1. \tag{22}$$

This implies that the most unstable orientation of a disturbance wavenumber vector is almost independent of its magnitude. Numerical solution of (7) over realistic ranges of parameter values indicated that orientations of the most unstable disturbance mode θ_{p}, of the smallest scale disturbance θ_{m} ((11) and (12)), and of the most unstable non-diffusive mode θ_0 ((15) and (16)) were always very close to each other (figure 1). In addition, typically θ_{p} is in between θ_0 and θ_{m}. Using this fact, (21) may be simplified as

$$\left.\begin{aligned} A_{\mathrm{p}} &= 2W_z \sec^2(2\theta_0)(\theta_{\mathrm{p}} - \theta_0)(1 + O(\phi)), \\ B_{\mathrm{p}} &= 2R_z \sec^2(2\theta_{\mathrm{m}})(\theta_{\mathrm{p}} - \theta_{\mathrm{m}})(1 + O(\phi)), \\ M_{\mathrm{p}} &= -2n_0(1 + O(\phi^2)), \quad N_{\mathrm{p}} = -2l_{\mathrm{m}}^2(1 + O(\phi^2)). \end{aligned}\right\} \tag{23}$$

A convenient equation for l_{p} may be obtained by substituting (23) in (7):

$$l_{\mathrm{p}} \approx \left[\frac{n_{\mathrm{p}}(n_{\mathrm{p}} - n_0)}{\tau}\right]^{\frac{1}{4}}. \tag{24}$$

From (10) and (14), neglecting terms of order $\phi\tau$ compared to one, it can be shown that

$$n_0 = \tau l_{\mathrm{m}}^2 - \tfrac{1}{2}\hat{\phi}\tau\left[rR_z + \frac{R_x^2 + rR_z^2}{(R_x^2 + R_z^2)^{\frac{1}{2}}}\right], \tag{25}$$

where $r = \alpha T_z^0/\beta S_z^0$. Now $\mathrm{d}\rho/\mathrm{d}z < 0$ implies $R_z(1-r) < 0$ (assuming $(r-1)\phi < 1$) and this fact can be used to prove that the factor within square brackets in (25) is always positive. Using (25) it can be shown that $B_{\mathrm{p}}/A_{\mathrm{p}}$ (equation (20)) is always real and of order $1/(\tau\phi)^{\frac{1}{2}} (\gg 1)$, and so long as $O(\tau/\phi) \leqslant 1$, l_{p}^2 is always positive. This fact and (18), (20) and (24) yield

$$n_{\mathrm{p}} = \tfrac{1}{2}\tau[R_z + (R_x^2 + R_z^2)^{\frac{1}{2}}](1 + O(\phi)), \tag{26}$$

$$l_{\mathrm{p}} = \left(\frac{\phi\tau}{4\Gamma}\right)^{\frac{1}{4}}\left\{[R_z + (R_x^2 + R_z^2)^{\frac{1}{2}}]\left(rR_z + \frac{R_x^2 + rR_z^2}{(R_x^2 + R_z^2)^{\frac{1}{2}}}\right)\right\}^{\frac{1}{4}}(1 + O(\phi)), \tag{27}$$

$$\theta_{\mathrm{p}} = \theta_{\mathrm{m}} + O\left(\frac{R_x}{R_z}(\tau\phi)^{\frac{1}{2}}\right). \tag{28}$$

Conditions for validity of (26)–(28) – i.e. $\alpha T_z^0/\beta S_z^2 = O(1)$; the ratio of τ (the ratio of effective molecular diffusivity of salt to the thermal diffusivity of the matrix) and

porosity of ϕ of the medium to be much smaller than unity, $O(\tau/\phi) \leqslant 1$; and the slope of isoconcentration lines not too steep (i.e. $W_x/W_z \leqslant O(1)$) – are satisfied in most practical situations. Notice that $l_p/l_m = O(\phi\tau)^{\frac{1}{4}}$ and $(n_p - n_0)/n_0 = O(\phi)$.

The fact that usually $\theta_p \approx \theta_m \approx \theta_0$ (since $|\theta_0 - \theta_m| \ll 1$) implies that the tradeoffs involved in determining the most unstable direction of fluid displacement are essentially the same in both the diffusive and the non-diffusive case (discussed earlier). By contrast the most unstable lengthscale is determined by diffusive effects. Diffusivity always decreases the difference between the temperature (salinity) of a displaced fluid parcel $\hat{T}(\hat{S})$, and that of the surrounding fluid $T_2(S_2)$. In particular, for small-scale disturbances (i.e. $l > l_m$) concentration perturbations get diffused away before buoyancy forces can displace the fluid by any significant distance. When $\tau \ll 1$, though each of $\alpha(T_2 - \hat{T})$ and $\beta(S_2 - \hat{S})$ are decreased by diffusive effects, the decrease in $\alpha(T_2 - \hat{T})$ is much larger than that in $\beta(S_2 - \hat{S})$, so that for some disturbance lengthscales there is a net increase in the difference between these two concentration differences, which corresponds to a net increase in the destabilizing buoyancy force. Thus the most unstable wavenumber l_p owes its existence to double-diffusive effects.

4.2. *Salt fingering and interleaving*

From (11), (12) and (28) it is clear that when the vertical Rayleigh number R_z is positive, the inclination of wavefronts (angle γ in figure 3) typically varies between $\frac{1}{4}\pi$ and $\frac{1}{2}\pi$. When $R_x = 0$ the disturbance velocity field consists of strictly vertical layers of fluid sliding past each other. In a Newtonian fluid similar disturbances correspond to the onset of *salt fingering* (Holyer 1983). As the ratio R_x/R_z increases, the inclination of these layers from the vertical monotonically increases up to the maximum inclination of 45°. When $R_z < 0$ the inclination of wavefronts typically varies between 0 and $\frac{1}{4}\pi$. When $0 < |R_x/R_z| \ll 1$ one obtains almost horizontal layers of fluid sliding past each other. *Interleaving* or 'tongues' of this form are also predicted in Newtonian fluids (Holyer 1983), and have been observed in the laboratory by Thorpe *et al.* (1969), Wirtz *et al.* (1972), Ruddick & Turner (1979) and Holyer *et al.* (1987). As $|R_x/R_z|$ increases, the inclination of these layers from the horizontal monotonically increases up to the maximum of 45°. Holyer *et al.* (1987) found indirect evidence that in a Newtonian fluid the slope of interleaving intrusions does increase with increase in the strength of horizontal gradients. For the same value of $|R_x/R_z|$ salt fingers are smaller in layer thickness (higher l_p) and more vigorous (higher n_p) than horizontal interleaving.

4.3. *Narrowness of the peak*

An estimate of the sharpness of variation in the growth rate (near the peak) with variation in the angle of the wavenumber vector may be obtained by examining the non-diffusive limit. Equations (13), (15) and (16) may be used to obtain the following alternative expression for the non-diffusive growth rate:

$$n = \tfrac{1}{2}(W_x^2 + W_z^2)^{\frac{1}{2}}[\cos(2\theta_0) + \cos(2\varpi)],$$

where $\varpi = \theta - \theta_0$. Obviously the sharpness of the peak with respect to θ is that of a sine wave with a period of π. This is similar to a Newtonian fluid (Holyer 1983). Flow visualization studies of Thorpe *et al.* (1969) suggest that sharpness of this order may be such that only modes with $\theta \approx \theta_p$ can be observed beyond an initial period of growth. An estimate of the narrowness of the peak with respect to the wavenumber is obtained by solving (7) for $\theta = \theta_m$. From figure 4 it is clear that as $\phi \to 0$ the growth

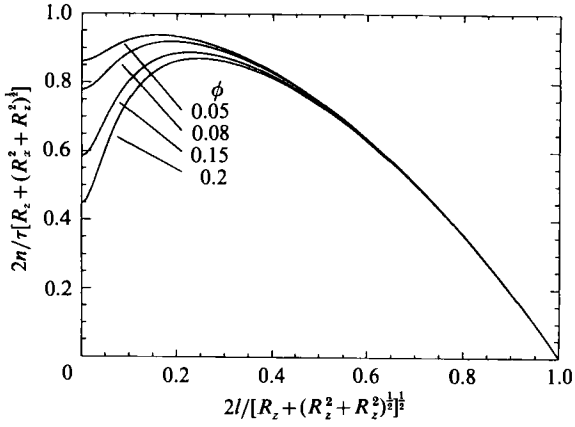

FIGURE 4. Dependence of the disturbance growth rate on wavenumber and porosity ($\theta = \theta_m$). $\tau = 0.01$, $\alpha T_x^0 = \beta S_x^0 = 1.2 \times 10^{-4}$, $\alpha T_z^0 = 5.7 \times 10^{-5}$ and $\beta S_z^0 = -6.5 \times 10^{-5}$. For the present scaling, qualitative features of this graph do not change with changes in concentration gradients. Note that $n = 0$ at $l = l_m$ (equation (10)).

rate is pretty much the same for all $l \leqslant l_p$. Obviously when $\phi \ll 1$ one may encounter a wide range of layer thicknesses. By contrast, in a Newtonian fluid the n *vs.* l peak is sharp enough that variation in layer thickness is small (Holyer 1983; Thorpe *et al.* 1969).

5. Fluxes of heat and salt

From (3), (4) and (6) the real parts of the stream function, temperature and salinity perturbations are found to be

$$\Psi'(x,z,t) = \psi_0 \, e^{nt} \cos(kx+mz), \tag{29}$$

$$T'(x,z,t) = \frac{mT_x^0 - kT_z^0}{\Gamma(n+k^2+m^2)} \psi_0 \, e^{nt} \sin(kx+mz), \tag{30}$$

$$S'(x,z,t) = \frac{mS_x^0 - kS_z^0}{\phi(n+\tau(k^2+m^2))} \psi_0 \, e^{nt} \sin(kx+mz), \tag{31}$$

where $k = l\cos\theta$ and $m = l\sin\theta$. Consequently perturbation fluxes of heat and salt in the horizontal and vertical directions are

$$F_{VT} = \left\langle -\frac{\partial \Psi'}{\partial x} T' \right\rangle = \frac{k(mT_x^0 - kT_z^0)}{2\Gamma(n+k^2+m^2)} \psi_0^2 \, e^{2nt}, \tag{32}$$

$$F_{VS} = \left\langle -\frac{\partial \Psi'}{\partial x} S' \right\rangle = \frac{k(mS_x^0 - kS_z^0)}{2\phi(n+\tau(k^2+m^2))} \psi_0^2 \, e^{2nt}, \tag{33}$$

$$F_{HT} = \left\langle \frac{\partial \Psi'}{\partial z} T' \right\rangle = -\frac{m(mT_x^0 - kT_z^0)}{2\Gamma(n+k^2+m^2)} \psi_0^2 \, e^{2nt}, \tag{34}$$

$$F_{HS} = \left\langle \frac{\partial \Psi'}{\partial z} S' \right\rangle = -\frac{m(mS_x^0 - kS_z^0)}{2\phi(n+\tau(k^2+m^2))} \psi_0^2 \, e^{2nt}, \tag{35}$$

where $\langle\,\rangle$ denotes spatial averaging over a wavelength. Notice that, on average,

diffusion does not contribute to perturbation fluxes of heat or salt. It can be shown that $(T_x^0 F_{HT} + T_z^0 F_{VT})$ and $(S_x^0 F_{HS} + S_z^0 F_{VS})$ are always negative, which implies that overall the perturbation fluxes always tend to reduce the basic-state concentration gradients. Also, the ratio of heat flux to salt flux $(F_{HT}/F_{HS} = F_{VT}/F_{VS})$ is positive for all permissible unstable disturbances (Appendix D).

When slopes of isoproperty lines are substantial, i.e. $|R_x/R_z| = O(1)$, then from (11), (12) and (31) it is clear that

$$S_x^0/S_z^0 = -\tan(2\theta_p)\,(1+O(\tau\phi)^{\frac{1}{2}}).$$

The above equation may be used to derive the following relations for modes with $\theta \approx \theta_p$:

$$F_{VS} = \frac{l^2 S_x^0}{4\phi(n+\tau l^2)\tan\theta_p}\psi_0^2 e^{2nt}, \tag{36}$$

$$F_{HS} = -\frac{l^2 S_x^0}{4\phi(n+\tau l^2)}\psi_0^2 e^{2nt}, \tag{37}$$

$$\frac{\alpha F_{HT}}{\beta F_{HS}} = \frac{\alpha F_{VT}}{\beta F_{VS}} = \left\{\frac{2\tan^2\theta_p + r(1-\tan^2\theta_p)}{\tan^2\theta_p}\right\}\frac{\phi(n+\tau(k^2+m^2))}{\Gamma(n+k^2+m^2)}, \tag{38}$$

where $r = \alpha T_z^0/\beta S_z^0$. From (11) and (12) it can be shown that $\tan\theta_m$, and hence $\tan\theta_p$ are always negative. Consequently F_{VS} and F_{HS}, corresponding to the peak growth rate, are negative too. The same conclusion applies to F_{HT} and F_{VT} (Appendix D). This implies that, so long as $S_x^0/S_z^0 = O(1)$, $(r-1)\phi/\Gamma < 1$ and $(d\rho/dz) < 0$ the horizontal components of fluxes are always from higher to lower concentration, while vertical components of perturbation fluxes are always downwards. This includes the intuitively uncomfortable scenario of vertical fluxes pumping salt (heat) from fresher (colder) fluid above to saltier (hotter) fluid below! Dynamical considerations require that the fluid velocity, and temperature and salinity fluctuations each change their sign from layer to layer. Hence though the fluid moves in alternate directions, the directions of heat and salt fluxes are limited to either being towards the third quadrant (the present case) or being towards the first quadrant (figure 3). In the later case the horizontal components of fluxes will always be against the basic-state horizontal gradients and, as will become clear later, will tend to increase the gravitational potential energy of the system. Obviously, the vertical flux component being always downwards is intuitively the more appealing of the two available alternatives. Putting $n_p \approx \tau l_m^2$ and $l_p^2 = O(l_m^2(\tau\phi)^{\frac{1}{2}})$ in (36)–(38) it can be seen that for the most unstable mode

$$F_{VS} \sim \frac{(\tau\phi)^{\frac{1}{2}}}{4\tan\theta_p} R_x \psi_0^2 e^{2nt}, \tag{39}$$

$$F_{HS} \sim -\tfrac{1}{4}(\tau\phi)^{\frac{1}{2}} R_x \psi_0^2 e^{2nt}, \tag{40}$$

$$\frac{\alpha F_{HT}}{\beta F_{HS}} = \frac{\alpha F_{VT}}{\beta F_{VS}} = O(\tau\phi)^{\frac{1}{2}} \leqslant 1, \tag{41}$$

where $\sim$ stands for equality within a factor of two or so. Obviously under typical conditions the perturbation salt flux is much stronger than the corresponding heat flux. By contrast in a Newtonian fluid, though salt is always transported more vigorously than heat, the flux ratio is of order one (Holyer 1983). Imhoff & Green (1988) obtained a flux ratio of order one in a porous medium using a sugar–salt

system. Though sugar and salt have different diffusivities, unlike heat and salt their advection rates through the porous medium are the same. Hence double-advective effects are absent in Imhoff & Green's experiment. Dynamically their experimental conditions are similar to double diffusion in a fluid. It is no surprise that their results are closer to Holyer's (1983) prediction than ours.

When slopes of isoproperty lines are small, i.e. $|R_x/R_z| \ll 1$, then for the salt fingering mode (i.e. $R_z > 0$) with $\theta \approx \theta_p$ the fluxes are

$$\left.\begin{aligned} F_{VS} &\approx -\frac{l^2 S_z^0}{2\phi(n+\tau l^2)}\psi_0^2 e^{2nt}, \\ F_{HS} &\approx -\frac{\delta l^2 S_z^0}{2\phi(n+\tau l^2)}\psi_0^2 e^{2nt}, \\ \frac{\alpha F_{HT}}{\beta F_{HS}} &= \frac{\alpha F_{VT}}{\beta F_{VS}} \approx \frac{\alpha T_z^0}{\beta S_z^0}\frac{\phi(n+\tau l^2)}{\Gamma(n+l^2)}, \end{aligned}\right\} \tag{42}$$

where $R_x/R_z = \delta \ll 1$. Notice that $R_z > 0$ implies $\alpha T_z^0 > \beta S_z^0 > 0$. Hence as before both vertical and horizontal components of salt and heat fluxes are negative. For the interleaving mode ($R_z < 0$) with $\theta \approx \theta_p$ the fluxes are

$$\left.\begin{aligned} F_{VS} &\approx -\frac{\delta l^2 S_x^0}{8\phi(n+\tau l^2)}\psi_0^2 e^{2nt}, \\ F_{HS} &\approx -\frac{l^2 S_x^0}{4\phi(n+\tau l^2)}\psi_0^2 e^{2nt}, \\ \frac{\alpha F_{HT}}{\beta F_{HS}} &= \frac{\alpha F_{VT}}{\beta F_{VS}} \approx \left(2-\frac{\alpha T_z^0}{\beta S_z^0}\right)\frac{\phi(n+\tau l^2)}{\Gamma(n+l^2)}, \end{aligned}\right\} \tag{43}$$

where $R_x/R_z = -\delta$. Notice that $R_z < 0$ implies $\beta S_z^0 < 0$, hence F_{VS}, F_{VT}, F_{HS} and F_{HT} are negative. Putting $n_p \approx \tau l_m^2$ and $l_p^2 = O(l_m^2(\tau\phi)^{\frac{1}{2}})$ in the above expressions for flux ratios one obtains

$$\frac{\alpha F_{HT}}{\beta F_{HS}} = \frac{\alpha F_{VT}}{\beta F_{VS}} = O(\tau\phi)^{\frac{1}{2}},$$

which is the same as (41), which implies that though vertical components of heat and salt fluxes may be countergradient, together they always tend to decrease the gravitational potential energy of the fluid.

The fact that vertical flux components are always downwards has important practical implications. For example pesticides or fertilizers (i.e. 'salt') applied on saturated soil will set up a vertical 'salinity' gradient ($S_z^0 > 0$) in the subsurface. Either simple overturning (if $d\rho/dz > 0$) or salt fingers (if the vertical temperature gradient is such that $d\rho/dz \leqslant 0$) will transport the contaminant downwards. With only thermohaline mechanisms occurring the soil will tend to accumulate all the contaminants at the bottom of the aquifer and never flush itself.

6. Later stages of the instability

Linear stability equations are valid only during the initial stages of the instability, i.e. for $nt \leqslant O(1)$. As nt increases further, nonlinear terms of the governing equations need to be taken into account. The full nonlinear governing equations include

$J(T', \Psi')$ and $J(S', \Psi')$ on the left-hand sides of (3) and (4) respectively, where the Jacobian is defined by

$$J(T', \Psi') = \frac{\partial \Psi'}{\partial z}\frac{\partial T'}{\partial x} - \frac{\partial \Psi'}{\partial x}\frac{\partial T'}{\partial z}.$$

The vorticity equation, (2), remains unchanged. Interestingly, for sinusoidal solutions of the form of (29) to (31) the Jacobian terms are identically zero, which implies that the linear solution ((29)–(31)) is also an exact solution of the nonlinear governing equations. The growth rate given by (7) also holds true for this solution. This theoretical property is also true for salt fingers (Huppert & Manins 1973) and horizontal interleaving (Holyer 1983) in Newtonian fluids. Unfortunately this solution does not take into account nonlinear interactions (through the Jacobian terms) between disturbances of different modes, and it does not provide any mechanism for the disturbances to evolve into steady states. Quite possibly this solution is not a realistic representation of the nonlinear evolution of disturbances.

Experiments by Thorpe *et al.* (1969), Wirtz *et al.* (1972), Ruddick & Turner (1979), Holyer *et al.* (1987) and others suggest that in a fluid the double-diffusive horizontal tongues (i.e. disturbances for the case $R_z < 0$), do not suffer any qualitative changes in flow pattern during their nonlinear evolution. We expect the same to hold true in a porous medium. By contrast, in a fluid the salt-fingering mode (i.e. disturbances for the case $R_z > 0$) may suffer secondary shear instabilities (Linden 1978). So long as the pore-scale Reynolds number is much smaller than one, flow in a porous medium is not expected to suffer shear instabilities. Because of the reduced possibility of secondary instabilities, salt fingers in a porous medium, unlike those in a liquid, are expected to retain their qualitative flow features during the process of nonlinear evolution. The above experiments also suggest that, so long as mean gradients of temperature and salinity are maintained constant, thermohaline disturbances eventually develop a steady-state flow pattern. It is important to know whether the steady-state linear solution is representative of the steady state reached by the disturbances subsequent to nonlinear evolution. Equation (8) (also (10)) implies that the linear solution can admit of a steady state only when the vertical and horizontal Rayleigh numbers formed with the layer thickness as the lengthscale are of order one. By contrast (27) implies that the most unstable layer thickness is such that the corresponding Rayleigh numbers are of $O(1/(\tau\phi)^{\frac{1}{2}})$ ($\gg 1$). So long as the basic state is held constant, it is quite unlikely that the thickness of a thermohaline layer would decrease by an order of magnitude through nonlinear interactions. Hence we believe that the steady-state linear solution is not a realistic representation of the steady state attained by disturbances.

While an accurate theoretical description of the nonlinear evolution of disturbances and the probable final steady state is beyond the scope of the present paper, some order of magnitude estimates of steady-state disturbance quantities are in order. To this end we need to make some intuitively acceptable closure assumptions regarding the steady state. Firstly, we assume that at steady state the disturbance salinity gradient ($|\nabla S'|$) is of the same order as the basic-state salinity gradient ($|\nabla S^0|$). Since temperature fluctuations are always much smaller than the corresponding salinity fluctuations ((30) and (31)) we cannot make a corresponding assumption regarding the temperature field. Secondly, we assume that the thickness of steady-state salt fingers or horizontal interleaving is of the same order as that of the most unstable linear mode (equation (27)). Thirdly, we assume that the appropriate lengthscale (L_u) characterizing spatial variation of the transport velocity is the thickness of the

thermohaline layer. Numerical analysis suggests this to be true for thermohaline layers in a Newtonian fluid (Wirtz *et al.* 1972) and for thermal convection in porous media (Trevisan & Bejan, 1987). Numerical and experimental studies of horizontal interleaving in fluids show that variations in the steady-state disturbance salinity field are typically limited to thin boundary layers (Wirtz *et al.* 1972). This is also true of high-Rayleigh-number thermal convection in porous media (Trevisan & Bejan 1987). Since Rayleigh numbers, based on the layer thickness, of the most unstable disturbances are larger than one ($O(1/(\tau\phi)^{\frac{1}{2}})$, our fourth assumption is that the lengthscale (L_S) characterizing spatial variations of the disturbance salinity field is much smaller than the layer thickness L_u.

Mathematically the above approximations are represented as

$$|\nabla S'| \sim |\nabla S^0|, \tag{44}$$

$$L_u \sim (\tau\phi)^{\frac{1}{4}}\left(\frac{k_\theta}{K\beta\nabla S^0}\right)^{\frac{1}{2}}, \tag{45}$$

$$L_S \ll L_u, \tag{46}$$

where a prime denotes disturbance quantities, L_u is the velocity lengthscale, L_S is the salinity length scale, K is the hydraulic conductivity, k_θ is the effective thermal diffusivity of the saturated medium, and $\sim$ denotes order of magnitude equality. Equation (45) is obtained from (27), assuming R_x/R_z and $\alpha T_z^0/\beta S_z^0$ are of order one. The vorticity and the steady-state salt conservation equations yield the following relations:

$$\frac{U}{L_u} \sim K\beta\nabla S', \tag{47}$$

$$\frac{U}{\phi}\nabla S^0 \sim \tau k_\theta \frac{\nabla S'}{L_S}, \tag{48}$$

where U is the magnitude of the transport velocity. Solving (44)–(48) one obtains

$$U \sim (\tau\phi)^{\frac{1}{4}}(Kk_\theta\beta\nabla S^0)^{\frac{1}{2}}, \tag{49}$$

$$L_S \sim (\tau\phi)^{\frac{1}{2}} L_u. \tag{50}$$

Equations (44)–(50) are in the dimensional form. Equations (49) and (50) are valid under the same conditions as (26)–(28). For a water-saturated medium with $k_p = 1$ darcy, $\tau\phi = 0.005$, $\beta\nabla S^0 = 1\%$ per 10 m, the right-hand side of (49) is approximately 25 cm/yr. For geological purposes this is a significant rate of transport. We expect that at the steady state $|\alpha\nabla T'| \ll |\beta\nabla S|$, hence thermal contributions are neglected in (47) and (49). Estimating $\alpha\nabla T'$ and the thermal lengthscale requires one additional closure assumption and the heat balance equation. Several alternative closure assumptions are possible, but we could not identify any one of them as being clearly superior to the others, so that we refrain from further discussion about the steady-state disturbance temperature field.

From (45) and (49) one may obtain an estimate of the steady-state salt flux per unit area as

$$F_S \sim UL_S\nabla S^0 \sim \phi(\tau k_\theta)\nabla S^0. \tag{51}$$

The above equation implies that the salt flux is linearly proportional to the basic-state concentration gradient. Thermal convection experiments in porous media do show this linear relationship (Elder 1967; Murray & Chen 1989). No data are

available for the thermohaline case. Equation (51) also implies that the salt flux due to double-diffusive instabilities is of the same order as that due to molecular diffusion (recall that τk_θ is the effective diffusivity of salt in the interstitial liquid). Numerical calculations by Wirtz *et al.* (1972) showed that in a Newtonian fluid the heat flux due to double-diffusive horizontal interleaving was indeed of the same order (though larger) as that of pure conduction.

Since we are treating the porous medium as a continuum it is important that the smallest lengthscale of the problem, L_S, be much larger than the r.m.s. grain size δ. Using the fact that the permeability k_p is of order $10^{-2}\phi\delta^2$ (Phillips 1991; §2.7) and (50) it can be shown that $L_S \gg \delta$ if

$$R_\delta \ll 100(\tau\phi)^{\frac{1}{2}}, \tag{52}$$

where $R_\delta (= g\beta\nabla S^0\delta^4/\tau k_\theta \nu)$ is the pore-scale Rayleigh number. The right-hand side of (52) is typically of order one. The above condition apparently implies that so long as the grain size is small enough to exclude the possibility of pore-scale thermohaline instabilities, the continuum approximation should hold. In a porous medium mechanical dispersion tends to increase the effective diffusivity of advectively transported salt. The increase in effective diffusivity is of the order $U\delta/\phi$ (Phillips 1991; §2.3). It can be shown that so long as (52) is true mechanical dispersion effects are negligible, i.e. $U\delta/\phi \ll \tau k_\theta$. Apparently thermohaline convection never becomes strong enough for mechanical dispersion to become important. This is the reason why mechanical dispersive effects were neglected in the steady-state salt balance equation (48). From (49) one obtains an estimate of the pore-scale Reynolds number:

$$Re_\delta \sim \frac{\tau}{Pr}\left[\frac{R_\delta}{10(\tau\phi)^{\frac{1}{2}}}\right]^{\frac{1}{2}}, \tag{53}$$

where $Re_\delta = U\delta/\phi\nu$, and $Pr(= \nu/k_\theta)$ is the Prandtl number. It is clear that so long as (52) is satisfied, Re_δ is much smaller than 1. This justifies using Darcy's law to represent momentum balance, and neglecting the possibility of any shear instability.

7. Summary

We have examined the consequences of the presence of horizontal concentration gradients on characteristics of thermohaline instabilities in a saturated homogeneous isotropic infinite porous medium, using the techniques of linear stability analysis. In the basic state horizontal gradients of temperature and salinity are taken to be mutually compensating, so that the basic-state fluid density does not vary horizontally. The fluid density is assumed not to increase with height (i.e. $\mathrm{d}\rho/\mathrm{d}z \leqslant 0$). The fluid is assumed to be incompressible (Boussinesq approximation). For a medium of infinite extent the appropriate length- and timescales are given by k_θ/K and k_θ/K^2 respectively (§2). Squire's theorem is found to hold (Appendix A); hence we consider only two-dimensional disturbances (equation (6)). The problem is governed by five non-dimensional parameters: W_x, W_z, R_x, R_z and τ (equation (5)). In the presence of horizontal property gradients (i.e. when $W_x, R_x \neq 0$) the situation is always unstable. In the absence of horizontal gradients the configuration is unstable only if the vertical Rayleigh number (R_z) is positive (equation (8)). It is also found that all oscillatory disturbances are damped, which implies that 'overstability' is not possible in the present case (§2). The largest unstable wavenumber (i.e. the smallest unstable lengthscale) is given by (10), and its orientation is given by (11) and (12).

In general the range of values of unstable wavenumber (l) and its orientation (θ) increase with increase in values of W_x, W_z, R_x and R_z (figure 1).

In §3 we show that the basic mechanism of the present instability is non-diffusive in nature. In a porous medium, assuming the solid matrix to be impervious to dissolved salts, the effective advection rates of heat and dissolved salts are different ((3) and (4)). Because of this difference any disturbance involving a horizontal component of displacement creates net horizontal density gradients, and thus destabilizes the predominantly hydrostatic force balance (equation (17)). This double-*advective* instability is similar to, but different from the double-*diffusive* instability observed in fluids. Though the double-advective effects are predominant, for disturbances of a certain lengthscale the double-diffusive effects do destabilize the situation even further. Hence the most unstable lengthscales ((19) and (27)) are determined by double-diffusive effects, double-advective effects being independent of the lengthscale (equation (13)). On the other hand the most unstable orientation of a disturbance wavenumber vector is determined almost exclusively by double-advective effects (equation (22)). We find that the most likely directions of fluid motion are limited to the first and third quadrants (where the positive z-axis points vertically upwards, and the basic-state temperature and salinity concentration increase to the right (figure 3)). When $R_z > 0$ the typical disturbance velocity field consists of almost vertical layers of fluid sliding past each other in opposite directions, i.e. *salt fingers*. When the vertical Rayleigh number is negative the fluid layers are almost horizontal, similar to the *interleaving* (or 'tongues') observed by Thorpe *et al.* (1969) and others (§4).

The ratio of heat flux to salt flux is positive for all permissible unstable disturbances (Appendix D), though typically the salt flux is much stronger than the corresponding heat flux (equation (41)). Regardless of the sign and magnitude of vertical concentration gradients the vertical flux components are always downwards. This result has practical implications in terms of 'irreversible' collection of pollutants at the bottom of aquifers. The perturbation fluxes always tend to reduce the basic-state concentration gradients, and the gravitational potential energy of the fluid. In §6 we make some tentative estimates regarding properties of these instabilities at the fully evolved state. Of particular interest are the estimates of the transport velocity, (49), and salt flux, (51). We find that under typical conditions (equation (52)) the pore-scale Reynolds number remains much smaller than 1 (equation (53)), and effects of mechanical dispersion remains negligible.

Appendix A. Squire's theorem

Combining Darcy's law with the incompressibility condition and the equation of state one obtains

$$\nabla^2 p' = \left(\alpha \frac{\partial T'}{\partial z} - \beta \frac{\partial S'}{\partial z}\right). \tag{A 1}$$

In the above equation the pressure is non-dimensionalized by $\mu k_\theta / k_p$, where μ is the dynamic viscosity of the fluid. The equations for conservation of heat and salt are

$$\left(\frac{\partial}{\partial t} - \nabla^2\right) T' = \frac{1}{\Gamma}\left[\frac{\partial p'}{\partial x} T^0_x + \left(\frac{\partial p'}{\partial z} - \alpha T' + \beta S'\right) T^0_z\right], \tag{A 2}$$

$$\left(\frac{\partial}{\partial t} - \tau \nabla^2\right) S' = \frac{1}{\phi}\left[\frac{\partial p'}{\partial x} S^0_x + \left(\frac{\partial p'}{\partial z} - \alpha T' + \beta S'\right) S^0_z\right]. \tag{A 3}$$

We assume the disturbances to be of the form

$$(p', T', S') = (p_0, t_0, s_0)\exp[nt + \mathrm{i}(k\cos\varpi x + k\sin\varpi y + mz)], \tag{A 4}$$

where ϖ is the angle between the horizontal component of the wavenumber vector and the direction of maximum thermohaline gradients (x-direction). In the notation of §2, $k = l\cos\theta$, $m = l\sin\theta$. Substituting (A 4) in (A 1)–(A 3) yields

$$t_0 = \frac{ik[m(\cos\varpi T_x^0) - kT_z^0]}{\Gamma m(n + k^2 + m^2)} p_0, \tag{A 5}$$

$$s_0 = \frac{ik[m(\cos\varpi S_x^0) - kS_z^0]}{\phi m(n + \tau(k^2 + m^2))} p_0, \tag{A 6}$$

$$n^2 + n[(1+\tau)l^2 - \tfrac{1}{2}(W_z(\cos 2\theta + 1) - (W_x\cos\varpi)\sin 2\theta)] + \left[\tau l^4 - \frac{\tau l^2}{2}(R_z(\cos 2\theta + 1) - (R_x\cos\varpi)\sin 2\theta)\right] = 0. \tag{A 7}$$

Comparing (A 5), (A 6) and (A 7) to (7), (32) and (33) it is clear that the dynamics of three-dimensional disturbances like (A 4) is identical to that of a two-dimensional disturbance with the strengths of horizontal gradients scaled down by a factor of $\cos\varpi$. Although we have not provided any formal proof that the growth rate monotonically increases with increase in $\beta S_x^0 (= \alpha T_x^0)$ for all possible two-dimensional disturbances, from (14) and (28) it is clear that so is the case for the most unstable modes.

Appendix B. Mode-dependent stability boundary

For a quadratic equation of the form

$$n^2 + bn + c = 0 \tag{B 1}$$

the two roots are given by

$$n_1 = q, \quad n_2 = c/q, \quad \text{where } q = -\tfrac{1}{2}[b + \mathrm{sgn}\,(b)\,(b^2 - 4c)^{\frac{1}{2}}]. \tag{B 2}$$

If both n_1 and n_2 are to be of the same sign (e.g. $\leqslant 0$) then we need

$$c \geqslant 0. \tag{B 3}$$

If both n_1 and n_2 are to be non-positive then we need $\mathrm{Re}(q) < 0$. From the definition of q it is clear that $\mathrm{Re}(q) < 0$ only if

$$b \geqslant 0. \tag{B 4}$$

For (7), conditions (B 3) and (B 4) imply

$$l^2 - \tfrac{1}{2}(R_z(\cos 2\theta + 1) - R_x\sin 2\theta) \geqslant 0, \tag{B 5}$$

$$l^2(1+\tau) - \tfrac{1}{2}(W_z(\cos 2\theta + 1) - W_x\sin 2\theta) \geqslant 0. \tag{B 6}$$

Equations (B 5) and (B 6) are equivalent to (8) and (9) respectively.

Appendix C. Decaying nature of oscillatory modes

For a quadratic equation of the form $n^2 + bn + c = 0$ to have complex roots it is necessary that $c > 0$, which for (7) implies

$$\mu R_x \geqslant R_z - k^2(1+\mu^2)^2, \tag{C 1}$$

where $\mu = \tan\theta$. From the discussion of Appendix B it is clear that real parts of both the roots of the quadratic equation will be negative only if $b > 0$ (in addition to $c > 0$), i.e.

$$\mu W_x \geqslant W_z - k^2(1+\tau)(1+\mu^2)^2. \tag{C 2}$$

A proof that (C 1) necessarily implies (C 2) will mean that all oscillatory modes decay with time. It can be shown that

$$W_x = R_x \frac{\tau(1-\phi/\Gamma)}{(1-\tau\phi/\Gamma)}, \tag{C 3}$$

$$W_z - R_z \frac{\tau(1-\phi/\Gamma)}{(1-\tau\phi/\Gamma)} = \frac{\mathrm{d}\rho/\mathrm{d}z}{\rho_0} \frac{(1-\tau)}{\Gamma(1-\tau\phi/\Gamma)}. \tag{C 4}$$

Using (C 3) and (C 4), (C 1) can be recast in the form

$$\mu W_x \geqslant W_z - k^2(1+\mu^2)^2 \frac{\tau(1-\phi/\Gamma)}{(1-\tau\phi/\Gamma)} - \frac{\mathrm{d}\rho/\mathrm{d}z}{\rho_0} \frac{(1-\tau)}{\Gamma(1-\tau\phi/\Gamma)}.$$

If $(\mathrm{d}\rho/\mathrm{d}z)(1-\tau)/[\rho_0\Gamma(1-\tau\phi/\Gamma)] < 0$ and $0 < \tau(1-\phi/\Gamma)/(1-\tau\phi/\Gamma) < (1+\tau)$ the above inequality implies

$$\mu W_x > W_z - k^2(1+\tau)(1+\mu^2)^2.$$

Hence satisfaction of (C 1) necessarily implies satisfaction of (C 2).

Appendix D. Sign of the flux ratio

From (32)–(35) one obtains

$$\frac{\alpha F_{HT}}{\beta F_{HS}} = \frac{\alpha F_{VT}}{\beta F_{VS}} = \frac{\alpha T_z^0}{\beta S_z^0} \left\{\frac{\mu(T_x^0/T_z^0)-1}{\mu(S_x^0/S_z^0)-1}\right\} \left[\frac{\phi(n+\tau l^2)}{\Gamma(n+l^2)}\right]. \tag{D 1}$$

It is obvious that for any unstable mode the factor within the square brackets on the right-hand size of (D 1) is positive. In addition $\mathrm{d}\rho/\mathrm{d}z < 0$ implies

$$\beta S_z^0 \leqslant \alpha T_z^0. \tag{D 2}$$

Equation (8) implies that for any unstable mode

$$\mu < \frac{R_z}{R_x} = \frac{S_z^0}{S_x^0} + O(\tau\phi), \tag{D 3}$$

where $\mu = \tan\theta$; also recall that $\beta S_x^0 = \alpha T_x^0 \geqslant 0$.

Case 1: $\mu > 0$. From (D 2) and (D 3) one obtains $0 < \beta S_z^0 < \alpha T_z^0$, also $\mu T_x^0/T_z^0 < \mu S_x^0/S_z^0 < 1$; that is both the denominator and the numerator within the braces in (D 1) are negative, hence the flux ratio is positive.

Case 2: $\mu < 0$ and $\beta S_z^0 > 0$. Obviously $\mu S_x^0/S_z^0 < 0$, and from (D 2) one obtains $\alpha T_z^0/\beta S_z^0 > 0$ and $\mu T_x^0/T_z^0 < 0$. Hence both the numerator and the denominator within the braces in (D 1) are negative, i.e. the flux ratio is positive.

Case 3: μ, βS_z^0, $\alpha T_z^0 < 0$. Equation (D 2) implies $|\alpha T_z^0| < |\beta S_z^0|$, and (D 3) implies $\mu S_x^0/S_z^0 > 1$. Hence $1 < \mu S_x^0/S_z^0 < \mu T_x^0/T_z^0$. That is both the numerator and the denominator within the braces in (D 1) are positive, hence the flux ratio is positive.

Case 4: μ, $\beta S_z^0 < 0$ and $\alpha T_z^0 > 0$. As in case 3, $\mu S_x^2/S_z^0 > 1$, hence the denominator within the braces is positive. By contrast $\mu T_x^0/T_z^0 < 0$, hence the numerator and the factor within the braces are negative. The fact that $\alpha T_z^0/\beta S_z^0$ is negative makes the flux ratio positive.

Cases 1 to 4 together cover all possible combinations. This also implies that for unstable modes temperature and salinity perturbations are always in phase.

REFERENCES

BENNETT, S. C. & HANOR, J. S. 1987 Dynamics of subsurface salt dissolution at the Welsh Dome, Louisiana Gulf Coast. In *Dynamical Geology of Salt and Related Structures* (ed. I. Lerche & J. J. O'Brien). Academic.

BISCHOFF, J. L. & ROSENBAUER, R. J. 1989 Salinity variations in submarine hydrothermal systems by layered double-diffusive convection. *J. Geol.* **97**, 613–623.

ELDER, J. W. 1967 Steady free convection in a porous medium heated from below. *J. Fluid Mech.* **27**, 29–48.

EVANS, D. G. & NUNN, J. A. 1989 Free thermohaline convection in sediments surrounding a salt column. *J. Geophys. Res.* **94**, 12413–12422.

GRIFFITHS, R. W. 1981 Layered double-diffusive convection in porous media. *J. Fluid Mech.* 102, 221–248.

HART, J. E. 1971 On sideways diffusive instability. *J. Fluid Mech.* **49**, 279–288.

HOLYER, J. Y. 1983 Double-diffusive interleaving due to horizontal gradients. *J. Fluid Mech.* **137**, 347–362.

HOLYER, J. Y., JONES, T. J., PRIESTLEY, M. G. & WILLIAMS, N. C. 1987 The effect of vertical temperature and salinity gradients on double-diffusive interleaving. *Deep-Sea Res.* **34**, 517–530.

HUPPERT, H. E. & MANINS, P. C. 1973 Limiting conditions for salt fingering at an interface. *Deep-Sea Res.* **20**, 315–323.

IMHOFF, P. T. & GREEN, T. 1988 Experimental investigation of double-diffusive groundwater fingers. *J. Fluid Mech.* **188**, 363–382.

LINDBLOM, S. 1986 Textural and fluid inclusion evidence for ore deposition in the Pb-Zn deposit at Laisvall, Sweden. *Econ. Geol.* **81**, 46–64.

LINDEN, P. F. 1978 The formation of banded salt finger structure. *J. Geophys. Res.* **83**, 2902–2912.

MURRAY, B. T. & CHEN, C. F. 1989 Double-diffusive convection in a porous medium. *J. Fluid Mech.* **201**, 147–166.

NIELD, D. A. 1968 Onset of thermohaline connection in a porous medium. *Wat. Resour. Res.* **3**, 553–560.

PALIWAL, R. C. & CHEN, C. F. 1980 Double-diffusive instability in an inclined fluid layer. Part 2. Stability analysis. *J. Fluid Mech.* **98**, 769–785.

PHILLIPS, O. M. 1991 *Flow and Reactions in Permeable Rocks.* Cambridge University Press, 286pp.

RUDDICK, B. R. & TURNER, J. S. 1979 The vertical length scale of double-diffusive intrusions. *Deep Sea. Res.* **26**, 903–913.

THORPE, S. A., HUTT, P. K. & SOULSBY, R. 1969 The effect of horizontal gradients on thermohaline convection. *J. Fluid Mech.* **38**, 375–400.

TREVISAN, O. V. & BEJAN, A. 1987 Mass and heat transfer by high Rayleigh number convection in a porous medium heated from below. *Intl J. Heat Mass Transfer* **30**, 2341–2356.

WIRTZ, R. A., BRIGGS, D. G. & CHEN, C. F. 1972 Physical and numerical experiments on layered convection in a density-stratified fluid. *Geophys. Fluid Dyn.* **3**, 265–288.